Performance Analysis of Dynamic Lightpath Configuration for Symmetric WDM Ring Networks

Takuji Tachibana and Shoji Kasahara

Abstract

In this paper, we propose a dynamic lightpath configuration method for WDM ring network. With this method, lightpaths are established according to the congestion state of node and are released after some holding time. The performance of the proposed method is evaluated in light and heavy traffic cases. In the light traffic case, a single node in WDM ring network is modeled as a multiple queueing system, while M/G/1/K and M/G/c/c queues are used for the heavy traffic case. In both cases, loss probability of packet flow and wavelength utilization factor are derived. We also explore the performance of our proposed method by simulation. Numerical examples show that our analytical models in both cases are useful to predict loss probability of packet flow and wavelength utilization factor. Moreover, in the light traffic case, it is shown that small holding time is effective even when lightpath establishment/release time is small.

Index Terms: Dynamic Lightpath Configuration, OADM, Queueing Model, Symmetric WDM Ring Network

I. Introduction

Optical add/drop multiplexer (OADM) selectively adds/drops wavelengths to establish lightpaths in WDM networks [4], [3], [5], [9], [13], [16], [18], [21]. Lightpath provides all-optical connection between any pair of OADMs (see Fig. 1). The number of available wavelengths is 16, 32, 64, 128 and so on, and the wavelengths to be added/dropped are pre-selected in each OADM [7], [14], [19]. Hence significant pre-deployment network planning is required to specify which wavelengths are to be added/dropped. Once the network design is determined, the design will not be changed unless network operator is willing to change the network design. When the traffic pattern changes frequently, the OADM degrades the performance of the network [23]. However, if wavelengths are dynamically allocated, high utilization of wavelengths and large throughput of packets are expected [2].

In terms of lightpath establishment in WDM network, the routing and wavelength assignment (RWA) problem that determines which lightpath should be established and which wavelength should be allocated has been considered. In general, traffic assumptions fall into two categories; static or dynamic. The RWA problem for static traffic is referred to as static lightpath establishment (SLE) problem and formulated as a mixed-integer linear program [17], [25].

Recently, dynamic wavelength allocation, dynamic routing, and dynamic lightpath establishment have been studied due to the rapid growth of the Internet. [8] has proposed wavelengths allocation algorithms for lightpath in ring network and analyzed the worst-case performance of the algorithm. [12] has considered a dynamic lightpath establishment algorithm with which a bandwidth guaranteed path with fast restoration is dynamically established. [20] has focused on WDM ring networks and evaluated the impact of dynamic lightpath establishment on blocking probability. [26] has

T. Tachibana is with the Graduate School of Information Science, Nara Institute of Science and Technology, Takayama 8916-5, Ikoma, Nara 630-0192, Japan (email:takuji-t@is.aist-nara.ac.jp).

S. Kasahara is with the Graduate School of Information Science, Nara Institute of Science and Technology, Takayama 8916-5, Ikoma, Nara 630-0101, Japan (email:kasahara@is.aist-nara.ac.jp).

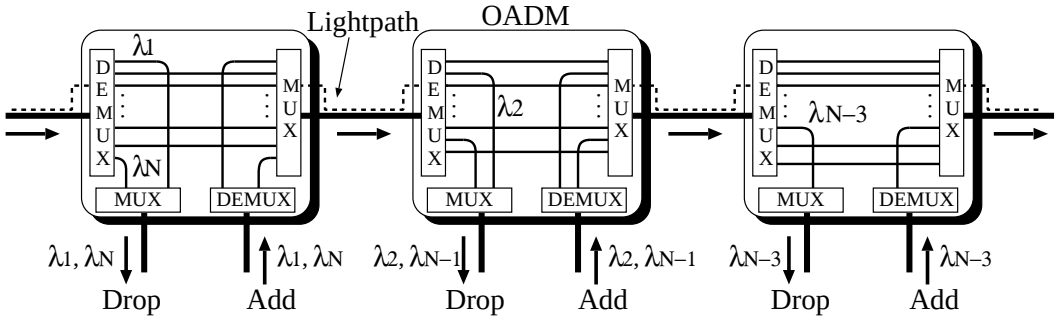

Fig. 1. Optical add/drop multiplexer.

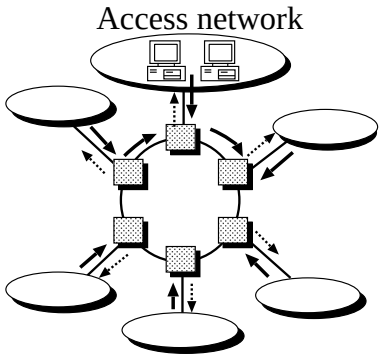

Fig. 2. Ring network model.

reviewed the control mechanism of dynamic lightpath establishment and compared the two control mechanisms based on link-state routing and distance-vector routing.

In this paper, we propose a dynamic lightpath configuration method for OADM equipped in WDM networks. With our proposed method, a lightpath is established according to the congestion state of node and kept being held during predefined extra holding time after the time instant that there are no packet flows to be transmitted in buffer for the lightpath. The lightpath is released if there are no arriving packet flows during the extra holding time.

Currently, WDM ring network shown in Fig. 2 is used for a backbone network as a substitute for conventional SONET/SDH ring network [7] and it is significant to analyze the performance of the proposed method in the ring network. For the performance analysis of the proposed method, we consider a WDM ring network under two traffic conditions: light and heavy ones. In the light traffic case, we model this system as a continuous-time Markov chain to take into account the lightpath establishment/release time.

In the heavy traffic case, established lightpaths are likely to be held for a while and lightpath establishment/release rarely occurs. Therefore we consider an M/G/1/K and multiple M/G/c/c queues for modeling a WDM ring network in the heavy traffic case.

In both cases, we consider packet flow which consists of consecutive packets and derive the loss probability of packet flow and wavelength utilization factor. With the analysis and simulation, we show how several parameters such as lightpath establishment/release time and holding time affect the performance measures.

The rest of the paper is organized as follows. Section 2 describes the lightpath configuration

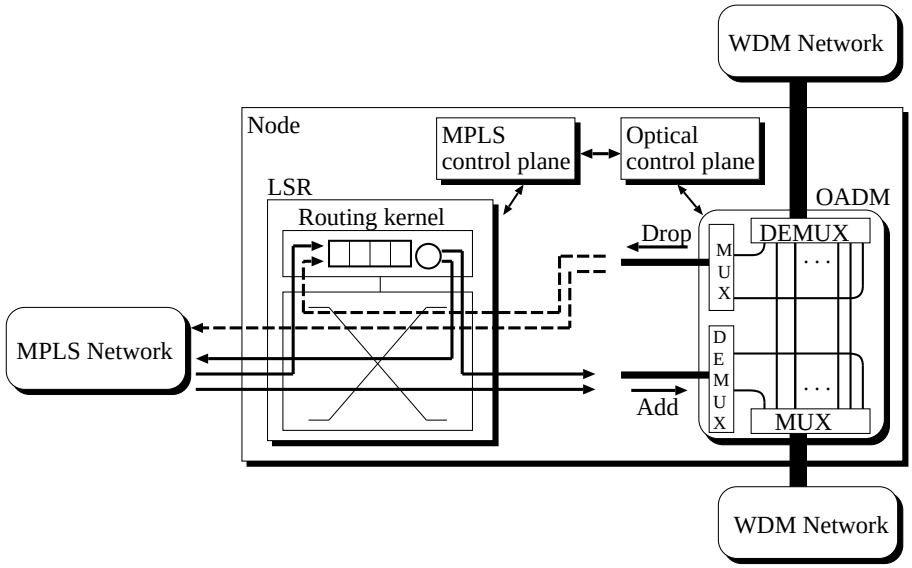

Fig. 3. Node architecture with OADM and LSR.

method, and in Section 3, the ring network model is represented. We show the performance analysis of our proposed method in light traffic case in Section 4. Then the performance analysis in heavy traffic case is presented in Section 5 and numerical examples are given in Section 6. Finally, conclusions are presented in Section 7.

II. Dynamic Lightpath Configuration Method

Each node in a WDM network consists of an OADM with MPLS control plane and a label switching router (LSR) with Layer 3 routing kernel (see Fig. 3). The LSR uses the label swapping paradigm and the OADM adds or drops a wavelength to establish a lightpath [1], [2], [6], [10]. The procedure of lightpath configuration is as follows (see Fig. 4).

For simplicity, we consider a tandem network with three nodes, namely, nodes A, B and C. Each node is connected to its own access network through LSR. Suppose $W+1$ wavelengths are multiplexed into an optical fiber in WDM network. Among $W+1$ wavelengths, W wavelengths are used to transmit data traffic and one is dedicated to distribute control traffic. Let w_i $(i = 0, \cdots, W-1)$ denote the ith wavelength for data traffic.

Among W wavelengths, the wavelength w_0 is used for the transmission to adjacent nodes (from A to B and from B to C in Fig. 4). We call the wavelength w_0 default path in the following. The default path only supports hop by hop label switched paths (LSPs). Packets transmitted with default path arrive at layer 3 routing kernel in LSR. At routing kernels in source and intermediate nodes, packets are routed to the next node. At routing kernel in destination node, on the other hand, packets are routed to the access network.

Other $W-1$ wavelengths are used for lightpaths which connect any pair of source and destination nodes. Those lightpaths are dynamically established/released between source and destination nodes according to congestion states in source and intermediate nodes along the path. An established lightpath contains multiple cut-through LSPs which have the same source and destination nodes.

When the first packet of newly arriving packet flow whose destination is node C arrives at the LSR of node A from access network, the LSR selects a wavelength with which the packet is transmitted.

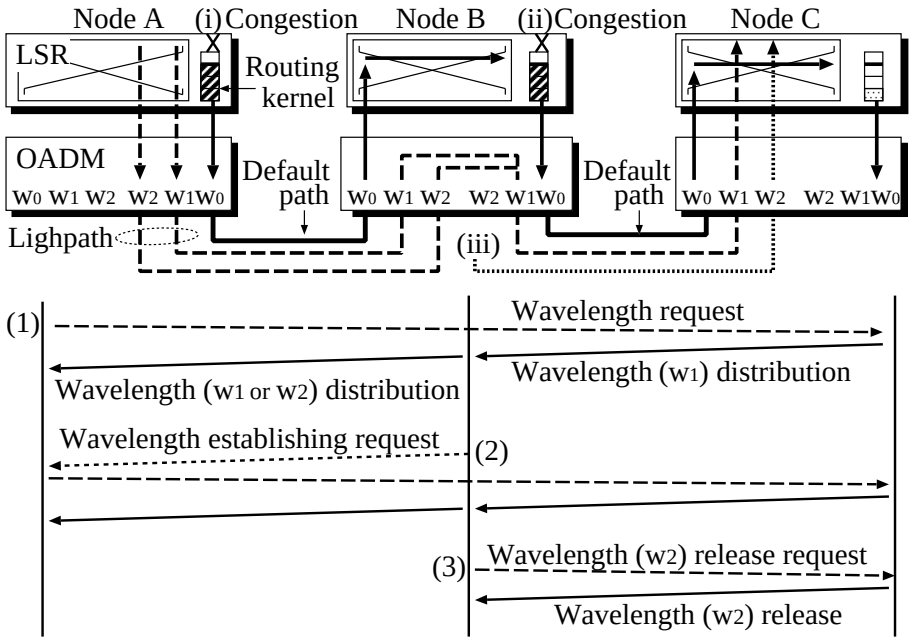

Fig. 4. Dynamic lightpath configuration.

If there exists an established lightpath between the two nodes, a new cut-through LSP is established in the lightpath for the transmission of the packet flow. If the establishment of the cut-through LSP fails due to the shortage of available bandwidth in the lightpath, the packet flow is forwarded to routing kernel again and transmitted to destination through default path [15].

In our proposed method, buffer in the routing kernel of LSR has a pre-specified threshold. If the amount of packet flows in the buffer becomes equal to or greater than the threshold, LSR regards the routing kernel as being in congestion and decides to establish a new lightpath between the source and destination nodes. This happens when the packet flow transmitted from nodes A to C triggers congestion at node A, or when it triggers congestion at node B.

In the former case, the MPLS control plane in node A requests the MPLS control plane in node C to establish a new lightpath with control signal (Fig. 4 (1)). Distributing network state information, MPLS control plane in each node has the latest information of lightpath configuration all the time. When the lightpath establishment request of node A arrives at node C, the MPLS control plane in node C searches an available lightpath for path BC. If wavelength w_1 is available for path BC, node C informs node B with control signal that w_1 is available, and then the OADM in node C drops w_1.

Subsequently, the MPLS control plane in node B searches an available wavelength for establishing lightpath between A and B. If w_1 is also available for path AB, node B informs node A of it. Otherwise, node B informs node A of another wavelength, say w_2. In the latter case, w_2 is converted to w_1 at node B for the transmission from A to C. If no wavelengths are available, this lightpath establishment fails.

Finally, the OADM in node A adds the wavelength of which node B informs. After the lightpath establishment is completed, a cut-through LSP is established in the lightpath.

In the case where congestion occurs at intermediate node B, the MPLS control plane in node B asks node A to request a new lightpath to node C (Fig. 4 (2)). Successive procedure is the same

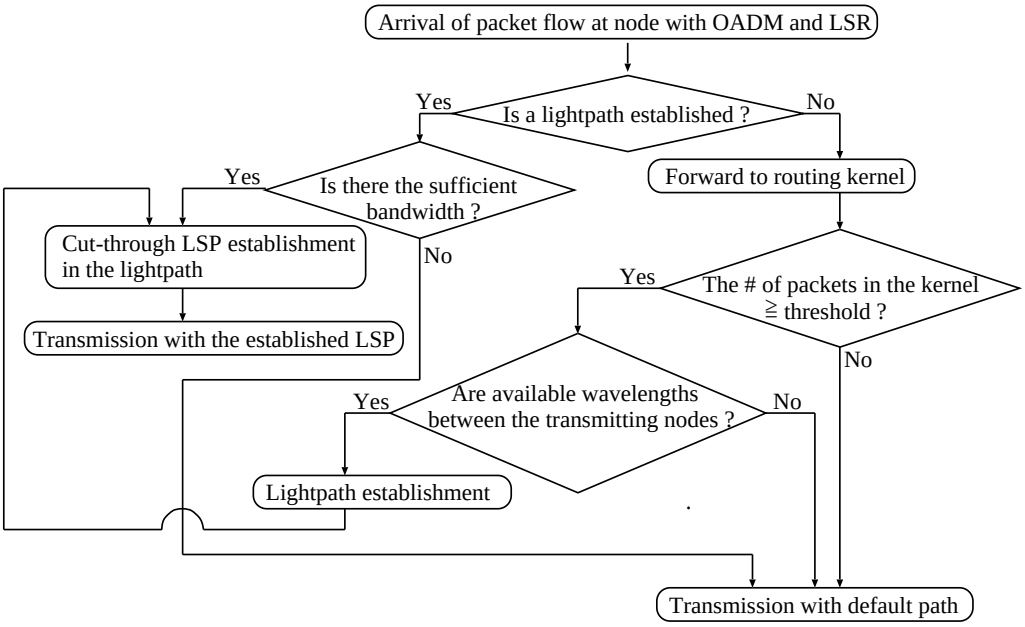

Fig. 5. Flowchart of lightpath establishment.

as the case (i).

When the lightpath becomes idle, the timer for the holding time during which the lightpath is kept being available starts. The lightpath is released if the holding time is over and no LSP is in the lightpath (Fig. 4 (iii), (3)).

The procedures of lightpath establishment and release are shown in Figs. 5 and 6, respectively.

III. Network Model

For the performance analysis of the proposed dynamic lightpath configuration, we consider a WDM ring network where L nodes are connected as shown in Fig. 2. Each node consists of OADM with MPLS control plane and LSR with layer 3 routing kernel, and lightpaths are established or released according to the dynamic lightpath configuration method. In addition, each node is connected to its own access network through LSR. For simplicity, we assume that multiple lightpaths between any pair of nodes are not permitted.

We assume that the number of wavelengths available at each node is W and that all wavelengths can be converted regardless of any wavelength pairs. One of W wavelengths is for default path and the others are for lightpaths which are dynamically established/released. $W-1$ wavelengths for lightpaths are numbered from 1 to $W-1$ and a lightpath is established with the wavelength which has the smallest number according to first-fit strategy.

Moreover we assume that the mean size of a packet flow is δ bits and that the destination of each packet flow is equally likely. This implies that the destination of packet flow which arrives at node i is node j ($j \neq i$) with probability $1/(L-1)$. Packet flows sent to some destination arrive at node according to a Poisson process with parameter λ. Since there are $L-1$ destinations for each node, packet flows arrive at node from its access network according to a Poisson process with parameter $(L-1)\lambda$. In this ring network, packet flows are transmitted in clockwise direction. Since the network is symmetric, we focus on a node in the network and consider the performance of our

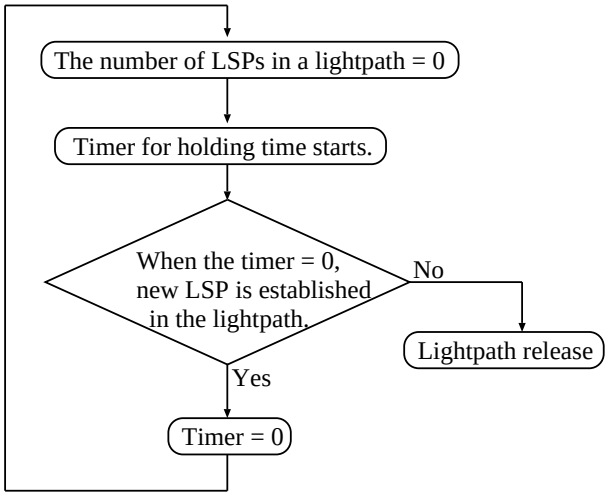

Fig. 6. Flowchart of lightpath release.

proposed method.

We assume that W wavelengths have the same bandwidth B bps, i.e., the bandwidth of established lightpath also has B bps. In addition, all established cut-through LSPs have the same bandwidth equal to B_l bps. Therefore, a lightpath supports up to $K_l = \lfloor B/B_l \rfloor$ cut-through LSPs.

Let K_r denote the capacity of a layer 3 routing kernel in LSR. Here, the capacity consists of a waiting room in which packet flows are stored for transmission, and a server where a packet flow is in transmission. Let T_h denote the pre-specified value of threshold for routing kernel. For simplicity of the analysis, we assume that the units of K_r and T_h are the number of packet flows.

IV. Performance Analysis in the Light Traffic Case

In this and the following sections, we analyze the performance of the dynamic configuration for WDM ring network. This section is devoted to the analysis in the light traffic case and the next section to that in the heavy traffic case.

A. System Model

In the light traffic case, the establishment/release of lightpaths may greatly affect the performance of the proposed method. Thus we consider a multiple queueing system under light traffic as shown in Fig. 7. In this network model, there are W queues in a node: one is for layer 3 routing kernel and the other $W-1$ queues are for lightpaths which are dynamically used according to the congestion of routing kernel. Here a lightpath supports K_l cut-through LSPs. In the light traffic case, we assume that the transmission times of packet flows for routing kernel and cut-through LSP are exponentially distributed with rates μ_r and μ_l, respectively. When the processing speed of the routing kernel is B_r bps and the size of a packet flow is δ bits, the mean transmission time of routing kernel is given by $1/\mu_r = \delta/B_r$ and that of cut-through LSP is given by $1/\mu_l = \delta/B_l$. Note that $B_r \leq B$ and $B_l \leq B$ where B is the bandwidth of a lightpath. We also assume that the establishment/release time and the holding time are exponentially distributed with rates p and h, respectively.

We have two kinds of packet flows that arrives at the node: one is from the access network and the other is from the previous node. As shown in the above, we assume that packet flows arrive at

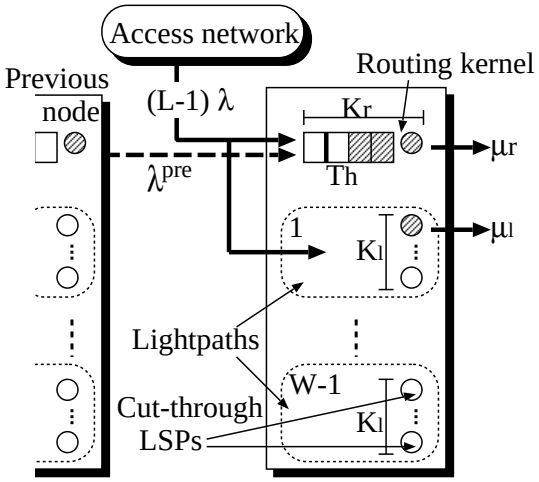

Fig. 7. Ring node model with light traffic.

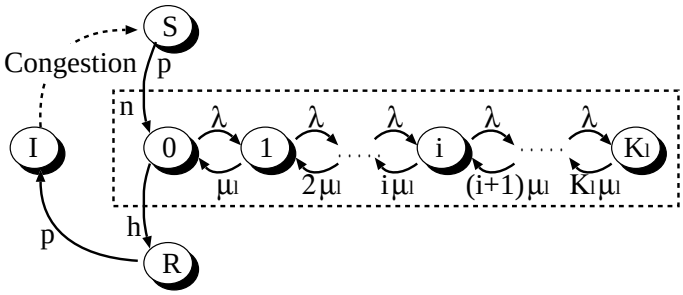

Fig. 8. State transition diagram for a lightpath.

the node from access network according to a Poisson process with rate $(L-1)\lambda$.

Next we consider packet flow traffic from the previous node. Since the packet flow arrives at the routing kernel depending on the congestion state and the queue size of the routing kernel is finite, our ring network is not an open Jackson queueing network. However, due to light traffic, we assume that arrival packet flow is hardly lost and most of packet flow arrives at a routing kernel and is transmitted through default path. Therefore we can approximate the arrival process from the previous node with the similar approach to the analysis of open Jackson network [11], [24].

The packet flows transmitted from the routing kernel in the previous node arrives at the routing kernel in the tagged node and then is routed to access network or the next node again. Let λ^{pre} denote the arrival rate at the routing kernel in the tagged node. Considering the transmissions originated from other $(L-1)$ nodes, we obtain

$$\lambda^{pre} = \frac{L(L-1)}{2}\lambda. \tag{1}$$

We assume that the packet flow arrival process from the previous node to the routing kernel is Poisson with rate λ^{pre}. Thus the whole arrival rate of packet flows at the node λ_{all} is given by

$$\lambda_{all} = (L-1)\lambda + \lambda^{pre} = \frac{(L+2)(L-1)}{2}\lambda. \tag{2}$$

B. Performance Analysis

Let l_i $(1 \leq i \leq W-1)$ denote the ith lightpath dynamically established/released at the node. We define the state of l_i at t as follows.

$$J_{l_i}(t) = \begin{cases} n, (n = 0, \cdots, K_l), & \text{if } l_i \text{ is busy and } n \text{ cut-through LSPs} \\ & \text{are established,} \\ I, & \text{if } l_i \text{ is idle,} \\ S, & \text{if } l_i \text{ is being established,} \\ R, & \text{if } l_i \text{ is being released.} \end{cases}$$

Let $N_r(t)$ denote the number of packet flows in the routing kernel at t. Then we define the state of the system at t as $(N_r(t),\ \boldsymbol{J}_l(t))$, where

$$\boldsymbol{J}_l(t) = (J_{l_1}(t), \cdots, J_{l_{W-1}}(t)). \tag{3}$$

The state transition diagram for l_i is illustrated in Fig. 8. Let U denote the whole state space of $(N_r(t),\ \boldsymbol{J}_l(t))$ and U_l the space comprised of $\boldsymbol{J}_l(t)$.

We define $M_l^B(N_r(t),\ \boldsymbol{J}_l(t))$ as the number of busy lightpaths in the state $(N_r(t),\ \boldsymbol{J}_l(t))$. $M_l^B(N_r(t),\ \boldsymbol{J}_l(t))$ is given by

$$M_l^B(N_r(t),\ \boldsymbol{J}_l(t)) = \sum_{i=1}^{W-1} \sum_{n=0}^{K_l} 1_{\{J_{l_i}(t)=n\}}, \tag{4}$$

where $1_{\{X\}}$ is the indicator function of event X. Similarly, we define $M_l^{K_l}(N_r(t),\ \boldsymbol{J}_l(t))$ as the number of lightpaths where K_l cut-through LSPs are established. Let $M_l^I(N_r(t),\ \boldsymbol{J}_l(t))$ denote the number of idle lightpaths. We have

$$M_l^{K_l}(N_r(t),\ \boldsymbol{J}_l(t)) = \sum_{i=1}^{W-1} 1_{\{J_{l_i}(t)=K_l\}}, \tag{5}$$

$$M_l^I(N_r(t),\ \boldsymbol{J}_l(t)) = \sum_{i=1}^{W-1} 1_{\{J_{l_i}(t)=I\}}. \tag{6}$$

In the remainder of this section, the argument t is omitted since we consider the system in equilibrium.

The transition rate from the state $(N_r,\ \boldsymbol{J}_l)$ is shown in Table I. In this table, $i_I^{\min}$ is defined as

$$i_I^{\min} = \min\{\, i\ ; J_{l_i} = I,\ 1 \leq i \leq W-1\}, \tag{7}$$

and $(N_r(t),\ \boldsymbol{J}_l(t))$ is omitted from $M_l^x(N_r(t),\ \boldsymbol{J}_l(t))$, $(x = B,\ K_l,\ I)$.

Finally, let $\pi(N_r,\ \boldsymbol{J}_l)$ denote the steady state probability of $(N_r,\ \boldsymbol{J}_l)$. $\pi(N_r,\ \boldsymbol{J}_l)$ is uniquely determined by equilibrium state equations and following normalized condition

$$\sum_{(N_r,\, \boldsymbol{J}_l) \in U} \pi(N_r,\ \boldsymbol{J}_l) = 1. \tag{8}$$

In Appendix A, we present equilibrium state equations in the case of $W = 2$.

TABLE I
STATE TRANSITION RATE IN RING NETWORK MODEL.

Number of idle lightpaths	Current state $(N_r,\ \boldsymbol{J}_l)$	Next state	Transition rate
$M_l^I > 0$	$N_r < T_h$	$(N_r+1,\ \boldsymbol{J}_l)$	$\lambda_{all} - (M_l^B - M_l^{K_l})\lambda$
	$T_h \le N_r < K_r$	$(N_r+1, \boldsymbol{J}_l),\ J_{l_{i_I^{\min}}} = S$	$\lambda_{all} - M_l^B\lambda$
	$T_h \le N_r < K_r$	$(N_r+1,\ \boldsymbol{J}_l)$	$M_l^{K_l}\lambda$
	$N_r = K_r$	$(N_r,\ \boldsymbol{J}_l),\ J_{l_{i_I^{\min}}} = S$	$\lambda_{all} - M_l^B\lambda$
	$N_r > 0$	$(N_r-1,\ \boldsymbol{J}_l)$	μ_r
$M_l^I = 0$	$N_r < K_r$	$(N_r+1,\ \boldsymbol{J}_l)$	$\lambda_{all} - (M_l^B - M_l^{K_l})\lambda$
	$N_r > 0$	$(N_r-1,\ \boldsymbol{J}_l)$	μ_r
State of lightpaths	Current state $(N_r,\ \boldsymbol{J}_l)$	Next state	Transition rate
$J_{l_i} = S$	$(N_r,\ \boldsymbol{J}_l)$	$(N_r,\ \boldsymbol{J}_l),\ J_{l_i} = 0$	p
$J_{l_i} = n$	$n < K_l$	$(N_r,\ \boldsymbol{J}_l + \boldsymbol{e}_i)$	λ
	$n > 0$	$(N_r,\ \boldsymbol{J}_l - \boldsymbol{e}_i)$	$n\mu_l$
	$n = 0$	$(N_r,\ \boldsymbol{J}_l),\ J_{l_i} = R$	h
$J_{l_i} = R$	$(N_r,\ \boldsymbol{J}_l)$	$(N_r,\ \boldsymbol{J}_l),\ J_{l_i} = I$	p

With $\pi(K_r,\ \boldsymbol{J}_l)$, the packet-flow loss probability P_{loss} is yielded as

$$P_{loss} = \sum_{(K_r, \boldsymbol{J}_l)\in U} \left\{1 - M_l^B(K_r,\ \boldsymbol{J}_l)\frac{\lambda}{\lambda_{all}} + M_l^{K_l}(K_r,\ \boldsymbol{J}_l)\frac{\lambda}{\lambda_{all}}\right\}\pi(K_r,\ \boldsymbol{J}_l). \tag{9}$$

We define P_{light} as the lightpath utilization factor and P_{wave} as the wavelength utilization factor. With $\pi(N_r,\ \boldsymbol{J}_l)$, P_{light} and P_{wave} are expressed as

$$P_{light} = \sum_{(N_r, \boldsymbol{J}_l)\in U} \sum_{i=1}^{W-1} 1_{\{0<J_{l_i}\le K_l\}}\frac{\pi(N_r,\ \boldsymbol{J}_l)}{W}, \tag{10}$$

$$P_{wave} = \sum_{(N_r, \boldsymbol{J}_l)\in U} \left\{1_{\{N_r>0\}} + \sum_{i=1}^{W-1} 1_{\{0<J_{l_i}\le K_l\}}\right\}\frac{\pi(N_r,\ \boldsymbol{J}_l)}{W}. \tag{11}$$

V. PERFORMANCE ANALYSIS IN HEAVY TRAFFIC CASE

In this section, we analyze the performance of our proposed method in the heavy traffic case.

A. System Model

Since the establishment/release of lightpaths rarely occurs and each node receives the same volume of traffic, we assume that each node maintains r lightpaths and that K_l cut-through LSPs are established in each lightpath all the time. As a result, we have an M/G/1/K_r queue for the layer 3 routing kernel and r M/G/K_l/K_l queues for established lightpaths, respectively (see Fig. 9). Note that $W - r - 1$ wavelengths are used for lightpaths established by other nodes.

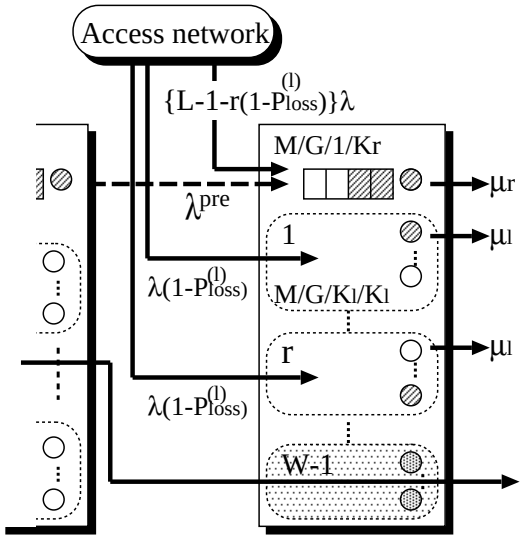

Fig. 9. Ring node model with heavy traffic.

In our approximation under heavy traffic, r plays an important role to obtain good estimates of performance measures. We give upper and lower bounds of r by considering the combination of lightpaths between any pairs of nodes in the ring network.

We define the length of lightpath as the number of links between source and destination nodes. r reaches its maximum when the number of lightpaths in the ring network is the largest and this occurs in the following way as shown in Fig. 10. First, establish lightpaths whose length equals one with one wavelength. Second, establish lightpaths whose length equals two with the least number of available wavelengths, and so on. Note that all nodes try to establish lightpaths equally in symmetric ring networks. It is easy to see that n wavelengths should be used if all nodes establish lightpaths with length equal to n. Since there are $W-1$ wavelengths, the maximum length n is given by

$$n = \max\{\, i : \frac{i(i+1)}{2} \leq W-1\}. \tag{12}$$

Each node tries to establish a lightpath with length equal to $n+1$, however, all nodes cannot establish them due to the shortage of available wavelengths.

Next we estimate the effect of wavelengths which are not used in the above procedure. In each node, the number of wavelengths which are not used for lightpaths is

$$W-1-\frac{n(n+1)}{2}.$$

There are L nodes and hence L links in the ring network. The number of lightpaths with length equal to $n+1$ in the network is given by

$$\frac{L}{n+1}\{W-1-\frac{n(n+1)}{2}\},$$

and hence the effect of the above per node is roughly estimated by

$$\frac{1}{n+1}\{W-1-\frac{n(n+1)}{2}\}.$$

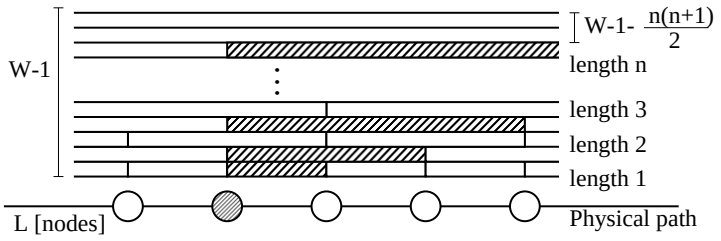

Fig. 10. Upper bound of the number of established wavelengths.

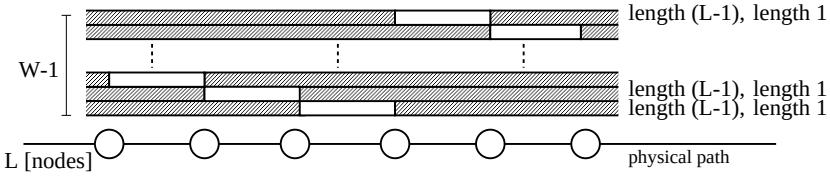

Fig. 11. Lower bound of the number of established wavelengths.

Combining the above results yields the upper bound of r as

$$r \leq n + \frac{1}{n+1}\{W - 1 - \frac{n(n+1)}{2}\}. \tag{13}$$

To obtain the lower bound of r, we consider a wasteful use of wavelengths. The most wasteful way is the establishment of lightpaths with length equal to $L-1$. In this case, we have two lightpaths in a wavelength: one is a path with length equal to $L-1$ and the other is that with length equal to one (see Fig. 11).

Since the number of lightpaths established in the network is $2(W-1)$, the effect per node is given by $2(W-1)/L$. That is,

$$r \geq \frac{2(W-1)}{L}. \tag{14}$$

From (13) and (14), we finally obtain the range of r as follows:

$$\frac{2(W-1)}{L} \leq r \leq n + \frac{1}{n+1}\{W - 1 - \frac{n(n+1)}{2}\}. \tag{15}$$

As is the case with light traffic case, we have two kinds of packet flow traffic that arrives at the node: one is from the access network and the other is from the previous node. First we consider packet flow traffic coming from access network. Since r lightpaths are established, a packet flow from access network arrives at the routing kernel or established lightpath. A packet flow arrives at the routing kernel according to a Poisson process with rate $(L-1-r)\lambda$ while it arrives at the established lightpath according to a Poisson process with rate λ.

The packet flow which arrives at a lightpath tries to establish a new cut-through LSP in the lightpath. If a new cut-through LSP is not established due to the shortage of bandwidth, the packet flow is forwarded to the routing kernel for the transmission with default path. Let $P_{loss}^{(l)}$ denote the probability that this cut-through LSP establishment fails at the packet-flow arriving

point. With M/G/K_l/K_l queueing model, $P_{loss}^{(l)}$ is given by

$$P_{loss}^{(l)} = \frac{(\lambda/\mu_l)^{K_l}/K_l!}{\sum_{k=0}^{K_l}(\lambda/\mu_l)^k/k!}, \tag{16}$$

where $1/\mu_l$ is the mean transmission time of a packet flow for a cut-through LSP.

Since the packet flow which fails in establishing a new cut-through LSP in the lightpath is forwarded to the routing kernel with rate $P_{loss}^{(l)}\lambda$, we assume that packet flows arrive at the routing kernel from its access network according to a Poisson process with rate $\{L-1-r(1-P_{loss}^{(l)})\}\lambda$.

Next we consider packet flow traffic from the previous node. Because the packet flow is transmitted from the previous node to the tagged node with default path all the time under heavy traffic, we assume that packet flow leaves the previous node according to Poisson process with rate μ_r.

Finally, the arrival rate of the packets at the routing kernel in the tagged node, λ_{all}, is given by

$$\lambda_{all} = \{L-1-r(1-P_{loss}^{(l)})\}\lambda + \mu_r. \tag{17}$$

B. Performance Analysis

In this subsection, we derive performance measures of the proposed method in the case of heavy traffic. As shown in Fig. 9, we consider an M/G/1/K_r queue and r M/G/K_l/K_l queues.

Let ρ_r and ρ_r' denote the offered and carried loads of routing kernel, respectively. We have

$$\rho_r = \frac{\lambda_{all}}{\mu_r}, \tag{18}$$

where λ_{all} is given by (17). We define π_o^r as the steady state probability that there are no packet flows in the routing kernel. Then ρ_r' is expressed as [22]

$$\rho_r' = \frac{\rho_r}{\pi_o^r + \rho_r}, \tag{19}$$

Since packet flow is lost only at routing kernel and hence loss probability P_{loss} is given by

$$P_{loss} = 1 - \frac{1}{\pi_0^r + \rho_r}. \tag{20}$$

Moreover wavelength utilization factor P_{wave} is expressed as

$$P_{wave} = \frac{\rho_r' + r\left\{1 - \frac{1}{\sum_{k=0}^{K_l}(\lambda/\mu_l)^k/k!}\right\}}{W}. \tag{21}$$

We can calculate π_o^r in a recursive procedure.

Remark. Since r is defined as the number of established lightpaths at node, r should take integer value. However, P_{loss} and P_{wave} are approximations and it is not clear whether non-integer r greatly affects P_{loss} and P_{wave}, or not. Therefore, for the calculations of P_{loss} and P_{wave}, we use (15) which takes real values.

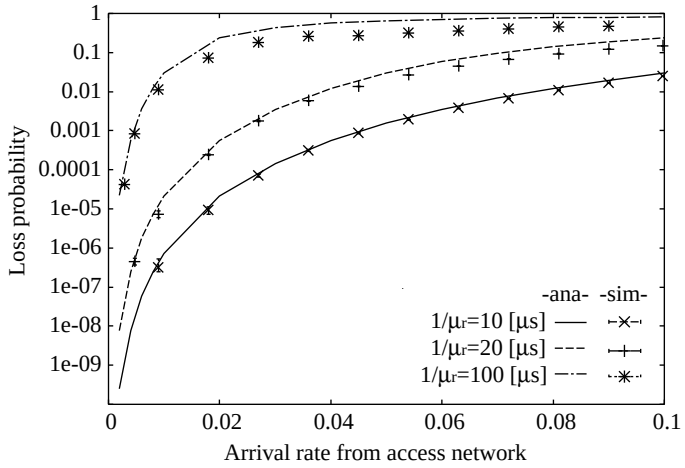

Fig. 12. Loss probability vs. arrival rate from access network in the light traffic case.

VI. Numerical Examples

In this section, we show numerical results calculated by approximation analysis and simulation. In simulation, we assume that the lightpath establishment/release time $1/p$ and the holding time $1/h$ are constant, while they are exponentially distributed with $1/p$ and $1/h$ in approximation analysis.

We assume that the bandwidth of a wavelength B is equal to 10 Gbps and each packet flow contains 10 packets whose sizes are 1,250 bytes. Hence the mean size of packet flow is $\delta = 100,000$ bits. We also assume that the size of packet flow is exponentially distributed with the mean.

A. Light Traffic Case

In this subsection, we show numerical results in the case of light traffic. Here, performance measures are calculated with the analytical results of Section IV.

A.1 Impacts of processing speed of routing kernel

First we consider how the processing speed of routing kernel affects packet-flow loss probability and wavelength utilization factor. Here we set $W = 4$, $K_r = 5$, $T_h = 3$ and $L = 10$. In this network, we assume that each wavelength supports only cut-through LSPs with fixed bandwidth $B_l = 2.5$ Gbps. Hence the number of cut-through LSPs in a lightpath $K_l = 4$ and the mean transmission time of a cut-through LSP $1/\mu_l = 2.5$ μs. In addition, we assume that both the mean lightpath establishment/release time $1/p$ and the mean holding time $1/h$ are the same and equal to 10 ms.

Figs. 12 and 13 show packet-flow loss probability and wavelength utilization factor against the arrival rate of packet flows in the cases of $1/\mu_r = 10$, 20 and 100 μs.

From Fig. 12, when the processing speed of routing kernel is 10 μs, loss probability calculated with approximation analysis is almost the same as that with simulation. On the other hand, when the processing speed of routing kernel becomes large, we can see the discrepancy between both results. This is because large processing time of routing kernel causes large loss probability and our assumption does not hold. Therefore the discrepancy becomes large as both the processing speed of routing kernel and the arrival rate increase. However, the discrepancy is still small and the results of approximation analysis give the upper bound for simulation ones. Therefore our approximation

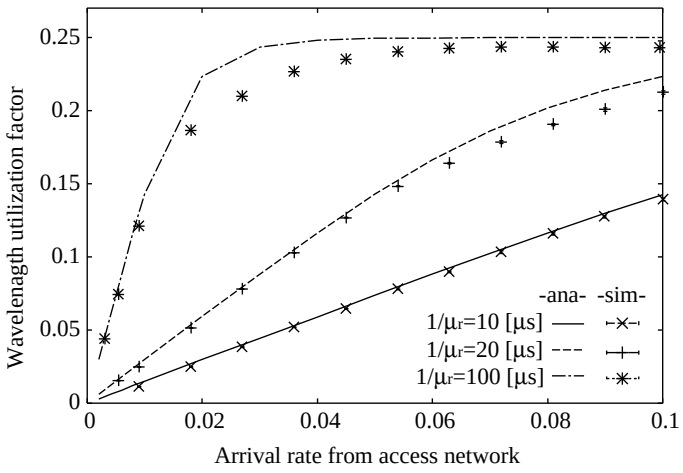

Fig. 13. Wavelength utilization factor vs. arrival rate from access network in the light traffic case.

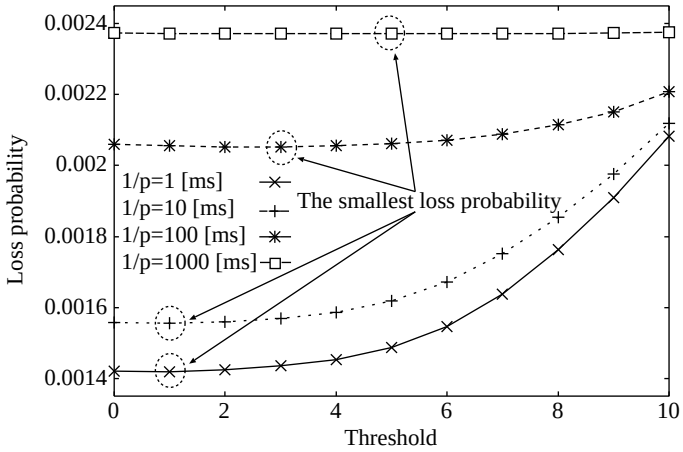

Fig. 14. Loss probability vs. threshold in the light traffic case.

analysis is useful for the calculation of loss probability in the light traffic case.

Fig. 13 illustrates wavelength utilization factor against the arrival rate of packet flow and we observe the same tendency as Fig. 12 in terms of the accuracy of the analysis.

In both figures, we observe that large processing time of routing kernel gives large loss probability and large wavelength utilization factor. This is because the large processing time of routing kernel causes congestion and this results in the increase of the number of established lightpaths.

A.2 Impact of threshold

Next we illustrate the impact of the congestion threshold on packet-flow loss probability and lightpath utilization factor in Figs. 14 and 15. These results are calculated from approximation analysis with $1/p$ set to 1, 10, 100, and 1000 ms when the bandwidth of a cut-through LSP is 10 Gbps. In addition, we indicate the optimal thresholds which achieve the smallest loss probability and the largest lightpath utilization factor in both figures. Here, we assume that $W = 4$, $K_r = 10$, and $L = 10$. Moreover, we assume that $(L-1)\lambda = 0.1$, $1/\mu_r = 10$ μs, and $1/h = 10$ ms.

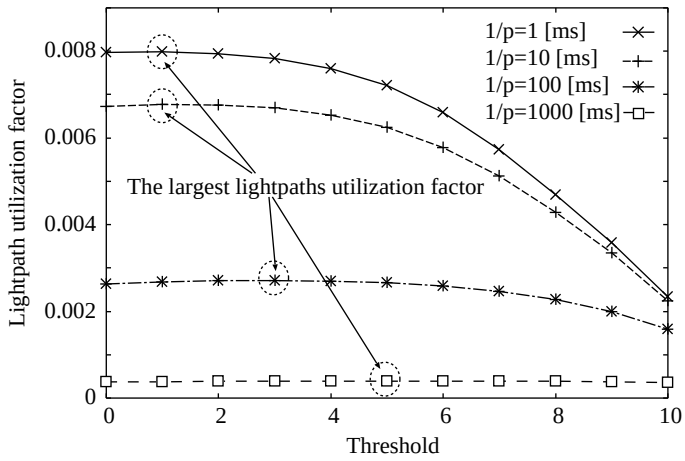

Fig. 15. Lightpath utilization factor vs. threshold in the light traffic case.

From Fig. 14, we find that values of T_h equal to 1, 1, 3, and 5 give the smallest loss probability in cases of $1/p = 1$, 10, 100 and 1000 ms, respectively. Moreover, in Fig. 15, the same threshold also gives the largest lightpath utilization factor. That is, the optimal thresholds in both figures are the same.

When threshold is smaller than the optimal threshold, congestion occurs frequently and this results in frequent lightpath establishment/release. Note that both loss probability and lightpath utilization factor do not degrade so much even though the wavelength can not be used during the lightpath establishment/release time.

On the other hand, as threshold becomes larger than the optimal threshold, congestion rarely occurs. If congestion does not occur, most of arriving packet flows are transmitted with default path. This causes large loss probability and small lightpath utilization factor. Consequently, it is important to design the threshold carefully in order to achieve small loss probability and large lightpath utilization factor.

A.3 Impact of lightpath establishment/release time and holding time

In this subsection, we consider how lightpath establishment/release time and holding time affect the loss probability and wavelength utilization factor under the proposed method for symmetric WDM ring network. Here we assume that $W = 4$, $K_r = 5$, $T_h = 1$ and $L = 10$. We also assume that $(L-1)\lambda = 0.05$, $1/\mu_r = 10$ μs, $B_l = 2.5$ Gbps and $1/\mu_l = 2.5$ μs.

Figs. 16 and 17 show loss probability and wavelength utilization factor, respectively, against lightpath establishment/release time in cases of $1/p = 0.1$, 1, 10 and 100 ms.

From Fig. 16, we observe that loss probability increases as lightpath establishment/release time $1/p$ becomes large. This is because the wavelength can not be used during the lightpath establishment/release time. On the other hand, we observe that the loss probability is not sensitive to the holding time. In particular, the loss probabilities except the case of $1/p = 100$ ms becomes almost constant when the holding time is larger than 20 ms. This implies that tuning the holding time is not so effective to decrease the loss probability when the lightpath establishment/release time is small.

In Fig. 17, we can see that wavelength utilization factor increases as lightpath establishment/release time becomes large. However, wavelength utilization factor shows the same tendency as loss prob-

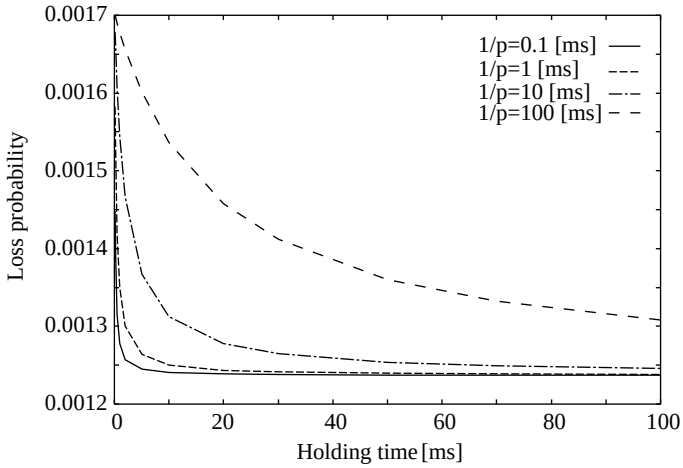

Fig. 16. Loss probability vs. holding time in the light traffic case.

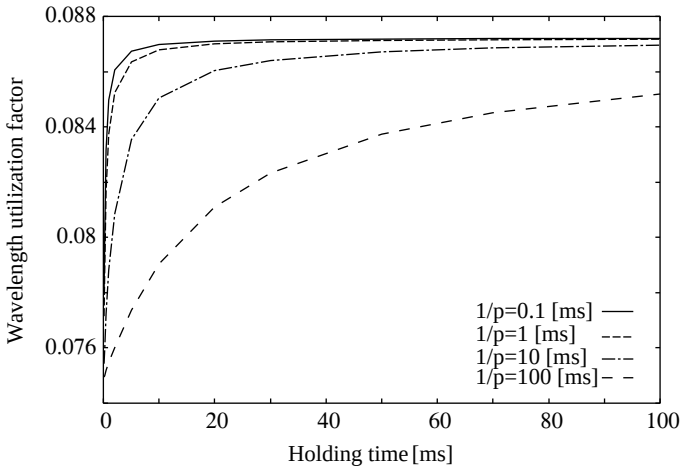

Fig. 17. Wavelength utilization factor vs. holding time in the light traffic case.

ability in Fig. 16. That is, when the lightpath establishment/release time is less than or equal to 10 ms, the holding time does not improve the wavelength utilization factor.

From the above observations, the small holding time is efficient for both loss probability and wavelength utilization factor even when the lightpath establishment/release time is in the order of 10 ms.

B. Heavy Traffic Case

In this subsection, we present numerical examples of loss probability and wavelength utilization factor for the heavy traffic case. We assume that $W = 4$, $K_r = 5$, $T_h = 3$ and $L = 10$. We also assume that $1/\mu_r = 10$ μs, $K_l = 4$ and $1/\mu_l = 2.5$ μs.

Figs. 18 and 19 illustrate the loss probability and wavelength utilization factor against arrival rate from access network, respectively.

In both figures, we set $1/h = 10$ ms, and calculate loss probability and wavelength utilization factor with $1/p$ set to 0.1, 1, 10, and 100 ms.

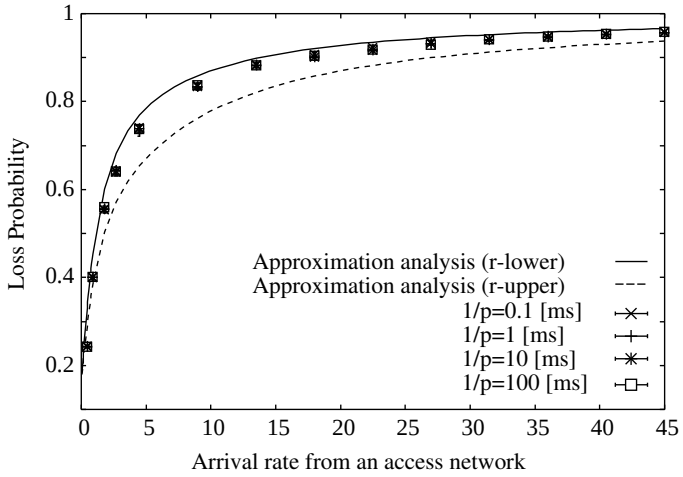

Fig. 18. Loss probability vs. arrival rate in the heavy traffic case, $1/h = 10$ ms.

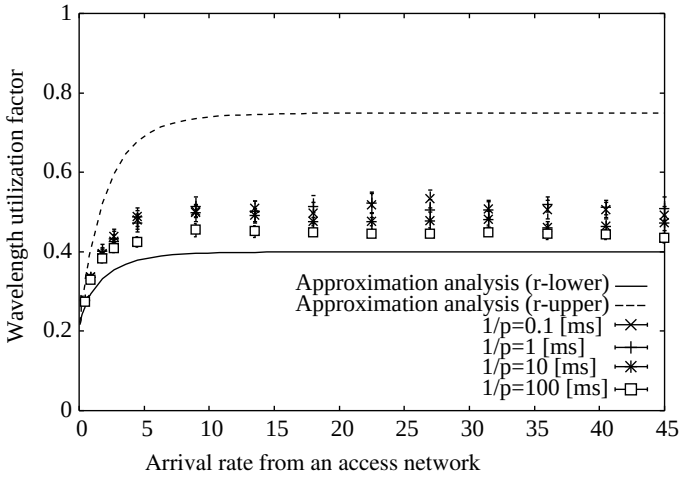

Fig. 19. Wavelength utilization factor vs. arrival rate in the heavy traffic case, $1/h = 10$ ms.

From Figs. 18 and 19, we observe that the values of simulation lie between the curves of the upper and lower bounds. Note that in Fig. 18, the upper bound value of r gives the lower bound of loss probability while the lower bound of r gives the upper bound of loss probability. In Fig. 19, however, the upper bound value of r gives the upper bound of wavelength utilization factors and vice versa.

In Fig. 18, simulation results close to the upper bound regardless of the establishment/release time. Note that the upper bound of the loss probability is calculated with the lower bound of r equal to $2(W-1)/L$. That is, the lower bound of r succeeds in the prediction of loss behavior under heavy traffic.

On the other hand, we observe in Fig. 19 that the simulation results become close to the lower bound when the establishment/release time becomes large. The discrepancy between upper and lower bounds, however, is large and our bounds fail in giving the good estimate for the wavelength utilization factor.

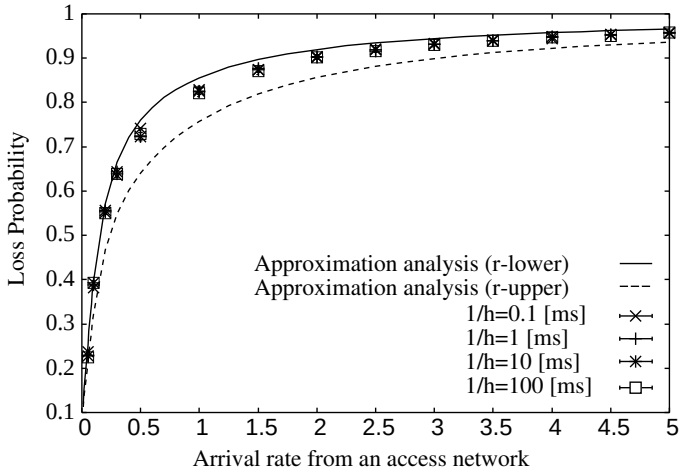

Fig. 20. Loss probability vs. arrival rate in the heavy traffic case, $1/p = 10$ ms.

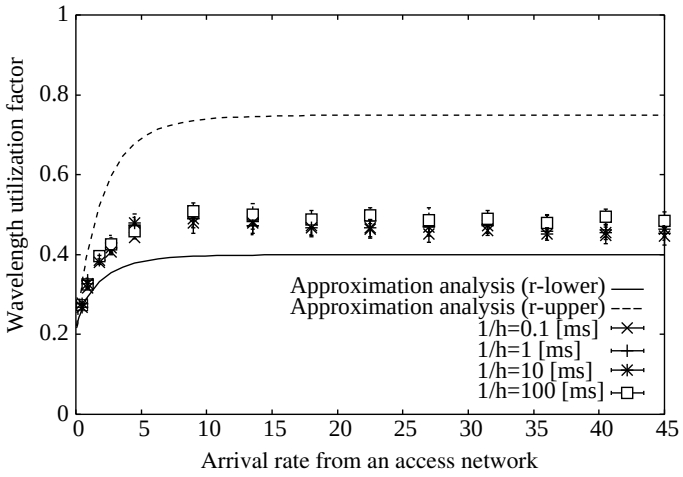

Fig. 21. Wavelength utilization factor vs. arrival rate in the heavy traffic case, $1/p = 10$ ms.

Figs. 18 and 19 show that loss probability and wavelength utilization factor do not change so much when lightpath establishment/release time becomes large. This is because the established lightpaths are not released frequently due to the heavy traffic.

Figs. 20 and 21 show the loss probability and wavelength utilization factor against arrival rate when the establishment/release time is 10 ms. In these figures, loss probability and wavelength utilization factor are calculated with the holding time set to 0.1, 1, 10, and 100 ms.

From Fig. 20, most of simulation results lie between upper and lower bounds except the case of holding time equal to one. As is the case with Fig. 18, the upper bound gives the good estimate of the loss probability. From Fig. 21, we also observe the same tendency as Fig. 19. Further improvement is needed for the estimation of the wavelength utilization factor.

VII. Conclusion

In this paper, we proposed a dynamic lightpath configuration method and analyzed the loss probability of packet flows and wavelength utilization factor under light and heavy traffic conditions for symmetric WDM ring networks.

Numerical results in light traffic case showed that our approximation analysis gives good estimates for loss probability and wavelength utilization factor. As for the design of the threshold in the proposed method, the optimal thresholds which give the smallest loss probability and the largest lightpath utilization factor can be obtained from the light traffic analysis. We also observed in the light traffic case that the small holding time is effective when the lightpath establishment/release time is in the order of 10 ms. In the heavy traffic case, we showed that our approximation analysis with lower bound of r is useful to estimate loss probability while the resulting estimates of wavelength utilization factor are not accurate. Further improvement of the approximation is needed for the well estimation of the wavelength utilization factor.

References

[1] D.O. Awduche, MPLS and Traffic Engineering in IP Networks, IEEE Commun. Mag. 37 (12) (1999) 42-47.

[2] D.O. Awduche, Y. Rekhter, Multiprotocol Lambda Switching: Combining MPLS Traffic Engineering Control with Optical Crossconnects, IEEE Commun. Mag. 39 (3) (2001) 111-116.

[3] P. Bonenfant, A.R. Moral, Optical Data Networking, IEEE Commun. Mag. 38 (3) (2000) 63-70.

[4] T. Chikama, H. Onaka, S. Kuroyanagi, Photonic Networking Using Optical Add Drop Multiplexers and Optical Cross-Connects, FUJITSU Sci. Tech. J. 35 (1) (1999) 46-55.

[5] I. Chlamtac, V. Elek, A. Fumagalli, C. Szabó, Scalable WDM Access Network Architecture Based on Photonic Slot Routing, IEEE/ACM Trans. Networking 7 (1) (1999) 1-9.

[6] R. Doverspike, J. Yates, Challenges for MPLS in Optical Network Restoration, IEEE Commun. Mag. 39 (2) (2001) 89-96.

[7] O. Gerstel, R. Ramaswami, G.H. Sasaki, Cost-Effective Traffic Grooming in WDM Rings, IEEE/ACM Trans. Networking 8 (5) (2000) 618-630.

[8] O. Gerstel, G.H. Sasaki, S. Kutten, R. Ramaswami, Worst-Case Analysis of Dynamic Wavelength Allocation in Optical Networks, IEEE/ACM Trans. Networking 7 (6) (1999) 833-846.

[9] N. Ghani, S. Dixit, T.S. Wang, On IP-over-WDM Integration, IEEE Commun. Mag. 38 (3) (2000) 72-84.

[10] A. Ghanwani, B. Jamoussi, D. Fedyk, P.A. Smith, N. Feldman, Traffic Engineering Standards in IP Networks Using MPLS, IEEE Commun. Mag. 37 (12) (1999) 49-53.

[11] L. Kleinrock, Queueing Systems, Volume I: Theory, Willey, New York, 1975.

[12] M. Kodialam, T.V. Lakshman, Dynamic Routing of Locally Restorable Bandwidth Guaranteed Tunnels using Aggregated Link Usage Information, in: Proc. INFOCOM 2001, 2001, pp. 376-385.

[13] M.W. McKinnon, H.G. Perros, G.N. Rouskas, Performance Analysis of Broadcast WDM Networks under IP Traffic, Perform. Eval. 36-37 (1999) 333-358.

[14] Y. Miyao, λ-Ring System: An Application in Survivable WDM Networks of Interconnected Self-Healing Ring Systems, IEICE Trans. Commun. E84-B (6) (2001) 1596-1604.

[15] S. Nakazawa, H. Tamura, K. Kawahara, Y. Oie, Performance Analysis of IP Datagram Transmission Delay in MPLS: Impact of Both Number and Bandwidth of LSPs of Layer 2, IEICE Trans. Commun. E85-B (1) (2002) 165-172.

[16] B. Ramamurthy, B. Mukherjee, Wavelength Conversion in WDM Networking, IEEE J. Select. Areas Commun. 16 (7) (1998) 1061-1073.

[17] R. Ramamurthy, K.N. Sivarajan, Routing and Wavelength Assignment in All-Optical Networks, IEEE/ACM Trans. on Networking 3 (5) (1995) 489-500.

[18] K. Sato, S. Okamoto, H. Hadama, Network Performance and Integrity Enhancement with Optical Path Layer Technologies, IEEE J. Select. Areas Commun. 12 (1) (1994) 159-170.

[19] R. Ramaswami, K.N. Sivarajan, Optical Networks: A Practical Perspective, Morgan Kaufmann Publishers, San Francisco, 1998.

[20] B. Schein, E. Modiano, Quantifying the Benefit of Configurability in Circuit-Switched WDM Ring Networks with Limited Ports per Node, IEEE J. Lightwave Tech. 19 (6) (2001) 821-829.

[21] K. Struyve, N. Wauters, P. Falcao, P. Arijs, D. Colle, P. Demeester, P. Lagasse, Application, Design, and Evolution of WDM in GTS's Pan-European Transport Network, IEEE Commun. Mag. 38 (3) (2000) 114-121.
[22] H. Takagi, A Foundation of Performance Evaluation, Volume 2: Finite Systems, Elsevier Science Publishers B, Amsterdam, 1993.
[23] W. Weiershausen, A. Mattheus, F. Küppers, Realisation of Next Generation Dynamic WDM Networks by Advanced OADM Design, in: D.W. Faulkner, A.L. Harmer (Eds.), WDM and Photonic Networks, IOS Press, Amsterdam, 2000, pp. 199-207.
[24] R.W. Wolff, Stochastic Modeling and the Theory of Queues, Prentice Hall, New Jersey, 1989.
[25] H. Zang, J.P. Jue, B. Mukherjee, A Review of Routing and Wavelength Assignment Approaches for Wavelength-Routed Optical WDM Networks, Opt. Net. Mag. 1 (1) (2000) 47-60.
[26] H. Zang, J.P. Jue, L. Sahasrabuddhe, R. Ramamurthy, B. Mukherjee, Dynamic Lightpath Establishment in Wavelength-Routed WDM Networks, IEEE Commun. Mag. 39 (9) (2001) 100-108.

Appendix

I. Equilibrium State Equations

For simplicity, we consider the case of $W = 2$. Then $\pi(N_r,\ J_{l_1})$'s satisfy the following equilibrium state equations.

- $J_{l_1} = I$: l_1 is idle.

$$\begin{aligned}
\lambda_{all}\pi(0,\ I) &= \mu_r\pi(1,\ I) + p\pi(0,\ R), && (22)\\
(\lambda_{all}+\mu_r)\pi(N_r,\ I) &= \lambda_{all}\pi(N_r-1,\ I) + \mu_r\pi(N_r+1,\ I)\\
&\quad + p\pi(N_r,\ R), \qquad (0 < N_r \le T_h), && (23)\\
(\lambda_{all}+\mu_r)\pi(N_r,\ I) &= \mu_r\pi(N_r+1,\ I)\\
&\quad + p\pi(N_r,\ R), \qquad (T_h < N_r < K_r), && (24)\\
(\lambda_{all}+\mu_r)\pi(K_r,\ I) &= p\pi(K_r,\ R). && (25)
\end{aligned}$$

- $J_{l_1} = S$: l_1 is being established.

$$\begin{aligned}
(\lambda_{all}+p)\pi(0,\ S) &= \mu_r\pi(1,\ S), && (26)\\
(\lambda_{all}+\mu_r+p)\pi(N_r,\ S) &= \lambda_{all}\pi(N_r-1,\ S)\\
&\quad + \mu_r\pi(N_r+1,\ S), \qquad (0 < N_r \le T_h), && (27)\\
(\lambda_{all}+\mu_r+p)\pi(N_r,\ S) &= \lambda_{all}\pi(N_r-1,\ S) + \lambda_{all}\pi(N_r-1,\ I)\\
&\quad + \mu_r\pi(N_r+1,\ S), \qquad (T_h < N_r < K_r), && (28)\\
(\mu_r+p)\pi(K_r,\ S) &= \lambda_{all}\pi(K_r-1,\ S) + \lambda_{all}\pi(K_r-1,\ I)\\
&\quad + \lambda_{all}\pi(K_r,\ I). && (29)
\end{aligned}$$

- $J_{l_1} = n$, $0 \le n \le K_l$: l_1 is busy.
  - $n = 0$

$$\begin{aligned}
(\lambda_{all}+h)\pi(0,\ 0) &= \mu_r\pi(1,\ 0) + \mu_l\pi(0,\ 1) + p\pi(0,\ S), && (30)\\
(\lambda_{all}+\mu_r+h)\pi(N_r,\ 0) &= (\lambda_{all}-\lambda)\pi(N_r-1,\ 0)\\
&\quad + \mu_r\pi(N_r+1,\ 0) + \mu_l\pi(N_r,\ 1)\\
&\quad + p\pi(N_r,\ S), \qquad (0 < N_r < K_r), && (31)\\
(\lambda+\mu_r+h)\pi(K_r,\ 0) &= (\lambda_{all}-\lambda)\pi(K_r-1,\ 0) + \mu_l\pi(K_r,\ 1)\\
&\quad + p\pi(K_r,\ S). && (32)
\end{aligned}$$

- $0 < n < K_l$

$$\begin{aligned}
(\lambda_{all} + \mu_l)\pi(0,\ n) &= \mu_r\pi(1,\ n) + \lambda\pi(0,\ n-1) \\
&\quad +\mu_l\pi(0,\ n+1), && (33)\\
(\lambda_{all} + \mu_r + \mu_l)\pi(N_r,\ n) &= (\lambda_{all} - \lambda)\pi(N_r - 1,\ n) \\
&\quad +\mu_r\pi(N_r + 1,\ n) + \lambda\pi(N_r,\ n-1) \\
&\quad +\mu_l\pi(N_r,\ n+1), \qquad (0 < N_r < K_r), && (34)\\
(\lambda + \mu_r + \mu_l)\pi(K_r,\ n) &= (\lambda_{all} - \lambda)\pi(K_r - 1,\ n) \\
&\quad +\lambda\pi(K_r,\ n-1) + \mu_l\pi(K_r,\ n+1). && (35)
\end{aligned}$$

- $n = K_l$

$$\begin{aligned}
(\lambda_{all} + \mu_l)\pi(0,\ K_l) &= \mu_r\pi(1,\ K_l) + \lambda\pi(0,\ K_l - 1), && (36)\\
(\lambda_{all} + \mu_r + \mu_l)\pi(N_r,\ K_l) &= \lambda_{all}\pi(N_r - 1,\ K_l) + \mu_r\pi(N_r + 1,\ K_l) \\
&\quad +\lambda\pi(N_r,\ K_l - 1), \qquad (0 < N_r < K_r), && (37)\\
(\mu_r + \mu_l)\pi(K_r,\ K_l) &= \lambda_{all}\pi(K_r - 1,\ K_l) + \lambda\pi(K_r,\ K_l - 1). && (38)
\end{aligned}$$

- $J_{l_1} = R$: l_1 is being released.

$$\begin{aligned}
(\lambda_{all} + p)\pi(0,\ R) &= \mu_r\pi(1,\ R) + h\pi(0,\ 0), && (39)\\
(\lambda_{all} + \mu_r + p)\pi(N_r,\ R) &= \lambda_{all}\pi(N_r - 1,\ R) + \mu_r\pi(N_r + 1,\ R) \\
&\quad +h\pi(N_r,\ 0), \qquad (0 < N_r < K_r), && (40)\\
(\mu_r + p)\pi(K_r,\ R) &= \lambda_{all}\pi(K_r - 1,\ R) + h\pi(K_r,\ 0). && (41)
\end{aligned}$$